Multi-Cell Random Beamforming: Achievable Rate and Degrees of Freedom Region

Hieu Duy Nguyen, Rui Zhang, and Hon Tat Hui

Abstract

Random beamforming (RBF) is a practically favourable transmission scheme for multiuser multi-antenna downlink systems since it requires only *partial* channel state information (CSI) at the transmitter. Under the conventional single-cell setup, RBF is known to achieve the optimal sum-capacity scaling law as the number of users goes to infinity, thanks to the *multiuser diversity* based transmission scheduling that eliminates the inter-user interference. In this paper, we extend the study on RBF to a more practical multi-cell downlink system subject to the additional inter-cell interference (ICI). First, we consider the case of *finite* user's signal-to-noise ratio (SNR). We derive a closed-form expression of the achievable sum rate with the multi-cell RBF, based upon which we show an asymptotic sum-rate scaling law as the number of users goes to infinity. Next, we consider the *high-SNR* regime and for tractable analysis assume that the number of users in each cell scales in a certain order with the per-cell SNR. Under this setup, we characterize the achievable degrees of freedom (DoF) (which is defined as the sum rate normalized by the logarithm of the SNR as the SNR goes to infinity) for the single-cell case with RBF. Furthermore, we extend the analysis to the multi-cell RBF case by characterizing the *DoF region*, which consists of all the achievable DoF tuples for all the cells subject to their mutual ICI. It is shown that the DoF region characterization provides useful insights on how to design the *cooperative* RBF scheme in a multi-cell system to achieve optimal throughput tradeoffs among different cells. Furthermore, our results reveal that the multi-cell RBF scheme achieves the "interference-free" DoF region upper bound for the multi-cell system, provided that the per-cell number of users has a sufficiently large scaling order with the SNR. This result confirms the optimality of the multi-cell RBF even without the full CSI at the transmitter, as compared to other full-CSI requiring transmission schemes such as *interference alignment*.

Index Terms

Random beamforming, degrees of freedom (DoF), DoF region, multiuser diversity, cellular network.

This work was presented in part at *IEEE International Conference on Acoustics, Speech, and Signal Processing (ICASSP)*, Kyoto, Japan, March 25-30, 2012.

The authors are with the Department of Electrical and Computer Engineering, National University of Singapore (email: {hieudn, elezhang, elehht}@nus.edu.sg).

I. Introduction

Recent studies have shown that multiuser (MU) multiple-input multiple-output (MIMO) or multi-antenna downlink systems can achieve much higher throughput than conventional single-user (SU) MIMO counterparts by simultaneously transmitting to multiple users with different spatial signatures. The sum-capacity and the capacity region of a single-cell MU-MIMO downlink system or the so-called MIMO broadcast channel (MIMO-BC) can be attained by the non-linear "Dirty Paper Coding (DPC)" scheme [1]-[3]. However, DPC requires high implementation complexity due to the non-linear successive encoding/decoding at the transmitter/receiver, and is thus not suitable for real-time applications. Other studies have proposed to use linear precoding schemes for the MIMO-BC, e.g., the block-diagonalization scheme [4], to reduce the complexity. However, such precoding schemes rely on the assumption of perfect channel state information (CSI) at the base station (BS) transmitter, which may not be realistic in practical cellular systems with a large number of users. Consequently, the study of quantized channel feedback for the MIMO-BC has recently been a very active area of research (see, e.g., [5] and the references therein).

In a landmark work [6], Viswanath *et al.* introduced a single-beam "opportunistic beamforming (OBF)" scheme for the MISO-BC, which exploits the multiuser diversity gain and requires only partial channel feedback to the BS. Since spatial multiplexing gain can be captured by transmitting with more than one random beams, the so-called "random beamforming (RBF)" scheme was also described in [6] and further investigated in [7]. The achievable sum rate with RBF in a single-cell system has been shown in [7], [8], which scales identically to that with the optimal DPC scheme assuming perfect CSI as the number of users goes to infinity, for any given user's signal-to-noise ratio (SNR). Essentially, this result implies that the intra-cell interference in a single-cell RBF system can be completely eliminated when the number of users is sufficiently large, and an "interference-free" MU broadcast system is attainable.

Although substantial investigations and/or extensions of the single-cell RBF have been pursued, there is very few works on the performance of the RBF scheme in a more realistic multi-cell system, where the inter-cell interference (ICI) becomes a dominant factor. It is worth noting that as the universal frequency reuse is more favourable in future generation cellular systems, ICI becomes a more severe issue as compared to the traditional case with only a fractional frequency reuse. A notable work is [9], in which the sum-rate scaling law for the multi-cell system with RBF has been shown to be similar to the single-cell result in [7], [8] as the number of per-cell users goes to infinity, regardless of the ICI. This result, albeit appealing, does not provide any insight on how to optimally design the RBF in an ICI-limited multi-cell system. In this paper, we aim to characterize the achievable rate for the multi-cell RBF scheme

by carefully analyzing the effects of ICI on the system throughput, for both the finite-SNR and high-SNR regimes.

It is worth noting that the multi-cell downlink system with ICI in general can be modelled as a Gaussian interference channel (IC). However, complete characterization of the capacity region of the Gaussian IC, even for the two-user case, is still an open problem [14]. An important development recently is the so-called “interference alignment (IA)” transmission scheme (see, e.g., [10]-[13] and the references therein). With the aid of IA, the maximum achievable degrees of freedom (DoF), which is defined as the sum rate normalized by the logarithm of the SNR as the SNR goes to infinity or the so-called “pre-log” factor, has been obtained for various types of ICs to provide useful insights on designing the optimal transmission for interference-limited MU systems. However, IA-based DoF analysis generally relies on the perfect CSI for all the intra- and inter-cell links. Furthermore, most of the studies on IA have not yet considered the practical case of a large number of users in each cell; as a result, the role of multiuser diversity in the DoF characterization remains unaddressed. Thus, in this paper, we characterize the achievable DoFs for the multi-cell system with RBF requiring only partial CSI at the BSs, when the number of per-cell users is typically a very large number.

Besides IA-based studies for the high-SNR regime, there is a vast body of works in the literature which investigated the multi-cell cooperative downlink precoding/beamforming at a given finite user’s SNR. These works are typically categorized based on two different types of assumptions on the level of BSs’ cooperation. For the case of “fully cooperative” multi-cell systems with global transmit message sharing across all the BSs, a virtual MIMO-BC channel is equivalently formed. Therefore, existing single-cell downlink precoding techniques can be applied (see, e.g., [15]-[17] and the references therein) with a non-trivial modification to deal with the per-BS power constraints as compared to the conventional sum-power constraint for the single-cell MIMO-BC case. In contrast, if transmit messages are only locally known at each BS, coordinated precoding/beamforming can be implemented among BSs to control the ICI to their best effort [18]-[20]. In [21]-[23], various parametrical characterizations of the Pareto boundary of the achievable rate region have been obtained for the MISO-IC with coordinated transmit beamforming and single-user detection (SUD).

Moreover, there have been recent results on the asymptotic analysis for the multi-cell MIMO downlink systems based on a large-system approach. The weighted sum-rate maximization and minimum rate maximization have been considered in [24], [25] and [26], respectively, for various multi-cell system setups. These works considered the regime in which the number of users per cell and the number of transmit antennas per BS both go to infinity at the same time with a fixed ratio. The major goal is to

apply random matrix theory to obtain “almost closed-form” numerical solutions that provide deterministic approximations for the optimal precoder designs at any given finite SNR. These results in turn lead to useful insights on the system design and performance optimization. Clearly, the asymptotic regime considered in the above works differs from that in this paper, where we consider the regime in which the number of per-cell users and the per-cell SNR both go to infinity by following a given prescribed order, while the number of transmit antennas at each BS is kept as a constant.

The main contributions of this paper are summarized as follows.

- **Finite-SNR Case**: In this case, we first consider the single-cell setup and show a new closed-form expression for the achievable average sum rate with RBF, based on the known distribution of the per-beam signal-to-interference-plus-noise ratio (SINR) given in [7]. We then study the multi-cell RBF and derive the SINR distribution in presence of the ICI, which is a non-trivial extension of the single-cell result in [7]. Based upon this new SINR distribution, we obtain a closed-form expression of the average sum rate in the multi-cell case, and characterize the asymptotic sum-rate scaling law as the number of users per cell goes to infinity, which is shown to be identical to that for the single-cell case [7] without the ICI. Notice that the same scaling law for the multi-cell RBF has been obtained in [9] based on an approximation of the SINR distribution, while in this paper we provide a more rigorous proof of this result using the exact SINR distribution.
- **High-SNR Case**: Although the achievable rates for the multi-cell RBF have been obtained for any given SNR with arbitrary number of users, such results do not provide any insight to the effects of the interference on the system throughput. This motivates us to investigate the multi-cell RBF for the asymptotic high-SNR regime, under the assumption that the number of users per cell scales in a given order with the per-cell SNR (a larger order indicates a higher user density in one particular cell). Under this setup, we first consider the single-cell case and derive the maximum DoF for the achievable sum rate with RBF, which is shown to be dependent on the user density and the number of transmit antennas, and attainable with the optimal number of random beams (data streams) employed at the transmitter. The DoF analysis thus provides a succinct description of the interplay between the multiuser diversity and spatial multiplexing gains achievable by RBF. We then seek to obtain a general characterization of the DoF region for the multi-cell RBF, which consists of all the achievable DoF tuples for all the cells subject to their mutual ICI. Different from the existing DoF region characterization based on IA [10] for the case of finite number of users, in this paper we address the case with an asymptotically large number of users that scales with SNR. Our

results reveal that coordination among the BSs in assigning their respective numbers of data beams based on different per-cell user densities is essential to achieve the optimal throughput tradeoffs among different cells. Moreover, we show that the DoF region by employing the multi-cell RBF coincides with the "interference-free" DoF region upper bound and thus the exact DoF region of a multi-cell downlink system, when the user densities in different cells are sufficiently large. This result is in sharp contrast with existing studies on the achievable DoF region with the full transmitter CSI obtained by schemes such as IA (see [10] and references therein).

The rest of the paper is organized as follows. Section II describes the multi-cell downlink model and the multi-cell RBF scheme. Section III studies the average sum rate for both single- and multi-cell RBF systems with finite SNR. Section IV characterizes the achievable DoF for single-cell RBF as well as the DoF region for multi-cell RBF at the high-SNR regime. Finally, Section V concludes the paper.

Notations: Scalars are denoted by lower-case letters, and vectors denoted by bold-face lower-case letters. The transpose and conjugate transpose operators are denoted as $(\cdot)^T$, and $(\cdot)^H$, respectively. $\mathbb{E}[\cdot]$ denotes the statistical expectation. $\mathbf{Tr}(\cdot)$ represents the trace of a matrix. The distribution of a circularly symmetric complex Gaussian (CSCG) random variable with zero mean and covariance σ^2 is denoted by $\mathcal{CN}(0,\sigma^2)$; and $\sim$ stands for "distributed as". $\mathbb{C}^{x\times y}$ denotes the space of $x \times y$ complex matrices.

II. System Model

This paper considers a multi-cell downlink system consisting of C cells, each of which has a BS with N_T antennas to coordinate the transmission with K_c single-antenna mobile stations (MSs), $K_c \geq 1$ and $c = 1, \cdots, C$. In the c-th cell, the c-th BS transmits $M_c \leq N_T$ orthonormal beams and selects M_c from K_c users for transmission at each time. We assume the channels to be flat-fading and constant over each transmission period of interest. For the ease of analysis, we also assume a "homogeneous" channel setup, in which the received baseband signal of user k in the c-th cell is given by

$$y_k^{(c)} = \boldsymbol{h}_k^{(c,c)} \sum_{m=1}^{M_c} \boldsymbol{\phi}_m^{(c)} s_m^{(c)} + \sum_{l=1,\ l\neq c}^{C} \sqrt{\gamma_{l,c}} \boldsymbol{h}_k^{(l,c)} \sum_{m=1}^{M_l} \boldsymbol{\phi}_m^{(l)} s_m^{(l)} + n_k^{(c)}, \tag{1}$$

where $\boldsymbol{h}_k^{(l,c)} \in \mathbb{C}^{1\times M_l}$ is the channel vector from the l-th BS to the k-th user of the c-th cell; it is assumed that all the elements of $\boldsymbol{h}_k^{(l,c)}$ are independent and identically distributed (i.i.d.) as $\mathcal{CN}(0,1)$; $0 \leq \gamma_{l,c} < 1$ stands for the distance-dependent signal attenuation from the l-th BS to any user in the c-th cell, $l \neq c$,

which is less than the assumed unit direct channel gain from the c-th BS[1]; $\boldsymbol{\phi}_m^{(c)} \in \mathbb{C}^{M_c \times 1}$ and $s_m^{(c)}$ are the m-th randomly generated beamforming vector of unit norm and transmitted data symbol from the c-th BS, respectively; it is assumed that each BS has the total sum power, P_T, i.e., $\mathbf{Tr}\left(\mathbb{E}[\boldsymbol{s}_c \boldsymbol{s}_c^H]\right) \le P_T$, where $\boldsymbol{s}_c = [s_1^{(c)}, \cdots, s_{M_c}^{(c)}]^T$; it is also assumed that the background noise is additive white Gaussian noise (AWGN), denoted by $n_k^{(c)} \sim \mathcal{CN}(0, \sigma^2)$, $\forall k, c$. In the c-th cell, the total SNR, the SNR per beam, and the interference-to-noise ratio (INR) per beam from the l-th cell, $l \neq c$, are denoted as $\rho = P_T/\sigma^2$, $\eta_c = P_T/(M_c\sigma^2)$, and $\mu_{l,c} = \gamma_{l,c} P_T/(M_l \sigma^2)$, respectively.

In this paper, we consider a multi-cell RBF scheme, in which all BSs in different cells are assumed to be able to implement the conventional single-cell RBF similarly to that given in [7] at the same time, which is described as follows:

- In the training phase, the c-th BS generates M_c orthonormal beams, $\boldsymbol{\phi}_1^{(c)}, \cdots, \boldsymbol{\phi}_{M_c}^{(c)}$, and uses them to broadcast the training signals to all users in the c-th cell. The total power of each BS is assumed to be distributed equally over M_c beams.
- Each user in the c-th cell measures the SINR value for each of M_c beams (shown in (2) below), and feeds it back to the corresponding BS.

$$\mathrm{SINR}_{k,m}^{(c)} = \frac{\frac{P_T}{M_c}\left|\boldsymbol{h}_k^{(c,c)}\boldsymbol{\phi}_m^{(c)}\right|^2}{\sigma^2 + \frac{P_T}{M_c}\sum_{i=1, i\neq m}^{M_c}\left|\boldsymbol{h}_k^{(c,c)}\boldsymbol{\phi}_i^{(c)}\right|^2 + \sum_{l=1, l\neq c}^{C}\gamma_{l,c}\frac{P_T}{M_l}\sum_{i=1}^{M_l}\left|\boldsymbol{h}_k^{(l,c)}\boldsymbol{\phi}_i^{(l)}\right|^2}$$

$$= \frac{\eta_c\left|\boldsymbol{h}_k^{(c,c)}\boldsymbol{\phi}_m^{(c)}\right|^2}{1 + \eta_c\sum_{i=1, i\neq m}^{M_c}\left|\boldsymbol{h}_k^{(c,c)}\boldsymbol{\phi}_i^{(c)}\right|^2 + \sum_{l=1, l\neq c}^{C}\mu_{l,c}\sum_{i=1}^{M_l}\left|\boldsymbol{h}_k^{(l,c)}\boldsymbol{\phi}_i^{(l)}\right|^2}, \quad (2)$$

  where $m = 1, \cdots, M_c$.
- The c-th BS schedules transmission to a set of M_c users at each time by assignning its m-th beam to the user with the highest SINR, i.e.,

$$k_m^{(c)} = \arg\max_{k\in\{1,\cdots,K_c\}} \mathrm{SINR}_{k,m}^{(c)}. \quad (3)$$

[1]This homogeneous channel setup is required to obtain the closed-form expressions for the achievable sum rates at finite SNRs, as will be detailed in Section III. However, the DoF region analysis for the asymptotically high-SNR regime as will be given in Section IV of the paper can be shown to hold even without the homogeneous channel assumption, i.e., the average signal attenuation from any BS to any user of any cell can take different values.

Thus, the achievable average sum rate in bits-per-second-per-Hz (bps/Hz) of the c-th cell is given by

$$R_{\text{RBF}}^{(c)} = \mathbb{E}\left[\sum_{m=1}^{M_c} \log_2\left(1 + \text{SINR}_{k_m^{(c)},m}^{(c)}\right)\right] = M_c \mathbb{E}\left[\log_2\left(1 + \text{SINR}_{k_1^{(c)},1}^{(c)}\right)\right]. \quad (4)$$

III. Achievable rate of multi-cell Random Beamforming: finite-SNR analysis

In this section, we study the achievable sum rate of a C-cell RBF system with finite SNR. We first derive a closed-form expression of the sum rate for the single-cell case, then extend the result to the multi-cell case subject to ICI, and finally investigate the asymptotic sum-rate scaling law as the number of users per cell goes to infinity.

A. Single-Cell RBF

We first consider the single-cell case, and drop the cell index c for brevity. Thus, (2) and (4) reduce to

$$\text{SINR}_{k,m} = \frac{\frac{P_T}{M}|\boldsymbol{h}_k\boldsymbol{\phi}_m|^2}{\sigma^2 + \frac{P_T}{M}\sum_{i=1,i\neq m}^{M}|\boldsymbol{h}_k\boldsymbol{\phi}_i|^2}, \quad (5)$$

$$R_{\text{RBF}} = M\mathbb{E}\left\{\log_2\left(1 + \max_{k\in\{1,\cdots,K\}} \text{SINR}_{k,1}\right)\right]. \quad (6)$$

The probability density function (PDF) and cumulative distribution function (CDF) of $S := \text{SINR}_{k,m}, \forall k, m$ can be expressed as [7]

$$f_S(s) = \frac{e^{-s/\eta}}{(s+1)^M}\left(M - 1 + \frac{s+1}{\eta}\right), \quad (7)$$

$$F_S(s) = 1 - \frac{e^{-s/\eta}}{(s+1)^{M-1}}, \quad (8)$$

where $\eta = P_T/(M\sigma^2)$ is the SNR per beam. A closed-form expression for the sum rate R_{RBF} is then given in the following lemma.

Lemma 3.1: The average sum rate of the single-cell RBF is given by

$$R_{\text{RBF}} = \frac{M}{\log 2}\sum_{n=1}^{K}(-1)^n\binom{K}{n}\left[\left(-\frac{n}{\eta}\right)^{n(M-1)}\frac{e^{n/\eta}Ei(-n/\eta)}{(n(M-1))!} - \sum_{m=1}^{n(M-1)}\left(-\frac{n}{\eta}\right)^{m-1}\frac{(n(M-1)-m)!}{(n(M-1))!}\right], \quad (9)$$

where $Ei(x) = \int_{-\infty}^{x}\frac{e^t}{t}dt$ is the exponential integral function.

Proof: Please refer to Appendix A. ■

Remark 3.1: It is worth making a comparison between Lemma 3.1 and other existing results in the literature as follows. Note that the sum-rate expression in Lemma 3.1 is exact, while only approximations

are given in [27] and [28]. Moreover, (9) involves the exponential integral function, which is more efficiently computable than the Gaussian hypergeometric functions given in [27] and [28]. However, the sum-rate approximations in [27] and [28] can directly lead to some desired asymptotic results, e.g., the sum-rate scaling law as $K \to \infty$, while (9) does not.

B. Multi-Cell RBF

For the single-cell RBF case, the SINR distributions given in (7) and (8) were obtained in prior work [7]. Now consider the multi-cell RBF case. If $\mu_{l,c} = \eta_c$, $\forall l \in \{1, \cdots, C\} \setminus \{c\}$, it is easy to see that the SINR distributions take the same forms as (7) and (8). However, if $\exists l \in \{1, \cdots, C\} \setminus \{c\}$ such that $\mu_{l,c} \neq \eta_c$, then the derivation of the SINR distributions in the multi-cell case becomes a new task due to the unevenly distributed ICI. To the best of the authors' knowledge, no closed-form expressions for the PDF and CDF of the SINR in this general case are available in the literature, while only approximated ones have been obtained (see, e.g., [9]). Therefore, in this subsection we first show a lemma on the exact SINR distributions for the multi-cell RBF, and then use them to investigate the achievable rate of this scheme.

Lemma 3.2: In the multi-cell RBF, the PDF and CDF of the SINR $S := \text{SINR}_{k,m}^{(c)}$, $\forall k, m$, are given by

$$f_S^{(c)}(s) = \frac{e^{-s/\eta_c}}{(s+1)^{M_c-1} \prod_{l=1, l\neq c}^{C} \left(\frac{\mu_{l,c}}{\eta_c} s + 1\right)^{M_l}} \left[\frac{1}{\eta_c} + \frac{M_c - 1}{s+1} + \sum_{l=1, l\neq c}^{C} \frac{M_l}{s + \frac{\eta_c}{\mu_{l,c}}}\right], \tag{10}$$

$$F_S^{(c)}(s) = 1 - \frac{e^{-s/\eta_c}}{(s+1)^{M_c-1} \prod_{l=1, l\neq c}^{C} \left(\frac{\mu_{l,c}}{\eta_c} s + 1\right)^{M_l}}. \tag{11}$$

Proof: Please refer to Appendix B. ■

It is worth noting that Lemma 3.2 nicely extends the single-cell results in (7) and (8), and clearly demonstrates the effect of ICI on the resulting SINR distributions. In Fig. 1, we compare the analytical and numerical SINR CDFs to confirm the validity of Lemma 3.2. We consider the SINR CDF of the first cell for two RBF systems with the following parameters: (1) $\eta_1 = 30$dB, $M_1 = 4$, $[\mu_{2,1}, \mu_{3,1}] = [-3, 3]$dB, $[M_2, M_3] = [2, 4]$; and (2) $\eta_1 = 20$dB, $M_1 = 6$, $[\mu_{2,1}, \mu_{3,1}, \mu_{4,1}] = [-3, 2, 3]$dB, $[M_2, M_3, M_4] = [2, 3, 4]$. It is observed that both analytical and numerical results match closely, thus justifying our derivation.

With Lemma 3.2, Lemma 3.1 is readily generalized to the multi-cell case in the following theorem.

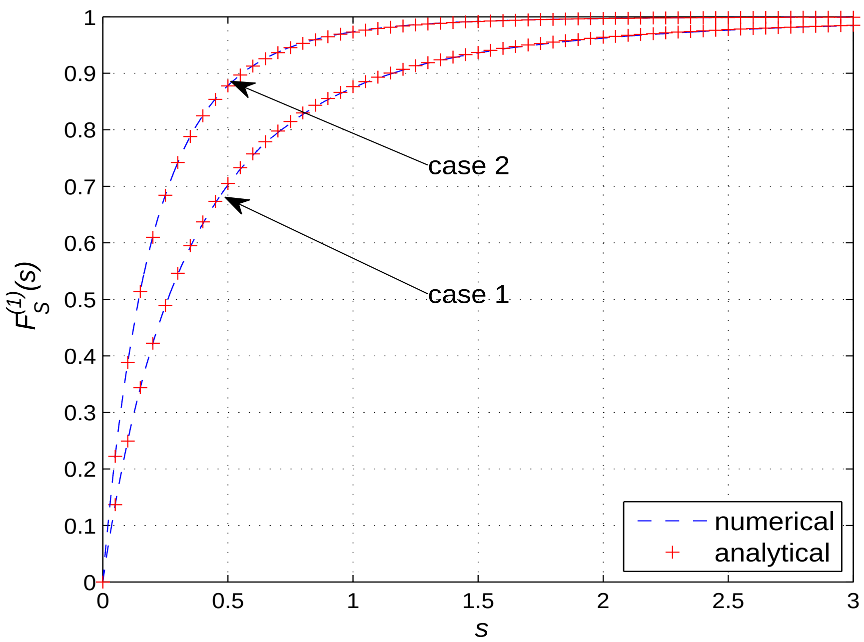

Fig. 1: Comparison of the analytical and numerical CDFs of the per-cell SINR.

Theorem 3.1: Denote the total sum rate of a C-cell RBF system as $\sum_{c=1}^{C} R_{\text{RBF}}^{(c)}$, where the individual sum rate of the c-th cell, $R_{\text{RBF}}^{(c)}$, is given by

$$
\begin{aligned}
R_{\text{RBF}}^{(c)} = \frac{M_c}{\log 2} \sum_{n=1}^{K_c} (-1)^n \binom{K_c}{n} \prod_{l=1, l\neq c}^{C} \left(\frac{\eta_c}{\mu_{l,c}}\right)^{nM_l} \times \\
\left\{ \sum_{p=1}^{n(M_c-1)+1} \frac{A_{n,c,p}}{(p-1)!} \left[e^{\frac{n}{\eta_c}} \left(-\frac{n}{\eta_c}\right)^{p-1} Ei\left(-\frac{n}{\eta_c}\right) - \sum_{m=1}^{p-1} \left(-\frac{n}{\eta_c}\right)^{m-1} (p-1-m)! \right] \right. \\
\left. + \sum_{l=1, l\neq c}^{C} \sum_{q=1}^{nM_l} \frac{A_{n,l,q}}{(q-1)!} \left[e^{\frac{n}{\mu_{l,c}}} \left(-\frac{n}{\eta_c}\right)^{q-1} Ei\left(-\frac{n}{\mu_{l,c}}\right) - \sum_{m=1}^{q-1} \left(-\frac{n}{\eta_c}\right)^{m-1} \left(\frac{\mu_{l,c}}{\eta_c}\right)^{q-m} (q-1-m)! \right] \right\},
\end{aligned} \tag{12}
$$

where $A_{n,c,p}$'s and $A_{n,l,q}$'s are the coefficients from the following partial fractional decomposition:

$$
\frac{1}{(x+1)^{n(M_c-1)+1} \prod_{l\neq c}^{C} \left(x + \frac{\eta_c}{\mu_{l,c}}\right)^{nM_l}} = \sum_{p=1}^{n(M_c-1)+1} \frac{A_{n,c,p}}{(x+1)^p} + \sum_{l=1, l\neq c}^{C} \sum_{q=1}^{nM_l} \frac{A_{n,l,q}}{\left(x + \frac{\eta_c}{\mu_{l,c}}\right)^q}, \tag{13}
$$

and given by [29, 2.102]:

$$A_{n,c,p} = \frac{1}{(n(M_c-1)-p+1)!} \frac{d^{n(M_c-1)-p+1}}{dx^{n(M_c-1)-p+1}} \left[\frac{1}{\prod_{l\neq c}^{C} \left(x+\frac{\eta}{\mu_l}\right)^{nM_l}} \right] \Bigg|_{x=-1}, \tag{14}$$

$$A_{n,l,q} = \frac{1}{(nM_l-q)!} \frac{d^{nM_l-q}}{dx^{nM_l-q}} \left[\frac{1}{(x+1)^{n(M_c-1)+1} \prod_{t\neq l,c}^{C} \left(x+\frac{\eta}{\mu_t}\right)^{nM_t}} \right] \Bigg|_{x=-\eta_c/\mu_{l,c}}. \tag{15}$$

Proof: Please refer to Appendix C. ■

In Fig. 2, we show the analytical and numerical results on the RBF sum rate as a function of the number of users for both single-cell and two-cell systems. We also compare the approximation obtained in [27], which is only applicable to the single-cell system. In the single-cell case, $M = N_T = 3$, $\eta = 20$ dB, while in the two-cell case, $K_1 = K_2$, $M_1 = M_2 = N_T = 3$, $\eta_1 = \eta_2 = 20$ dB, $\mu_{2,1} = 6$ dB, and $\mu_{1,2} = 10$ dB. It is observed that the approximation [27, (17)] is only an upper bound of the achievable sum rate. In contrast, the sum-rate expressions in (9) and (12) are observed to be very accurate. Thus, it is feasible to use Theorem 3.1 to characterize all the sum-rate tradeoffs among different cells in a multi-cell RBF system, which leads to the achievable rate region. However, such a characterization requires intensive computations, and does not provide any useful insight. In Section IV, we adopt an alternative approach based on the DoF region to provide a more efficient as well as insightful tradeoff analysis for the multi-cell RBF.

C. Asymptotic Sum Rate as $K_c \to \infty$

It is worth noting that a conventional asymptotic investigation of RBF is to consider the case when the number of users per cell approaches infinity for a given finite SNR. Consider the single-cell RBF case with $M \leq N_T$ transmit beams and K single-antenna users. The scaling law of the sum rate is shown to be $M \log_2 \log K$ as $K \to \infty$ with any fixed SNR, ρ, in [7], [8]. An attempt to extend this result to the multi-cell RBF case has been made in [9] based on an approximation of the SINR's PDF (which is applicable if the SNR and INRs are all roughly equal), by showing that the same asymptotic sum-rate $M_c \log_2 \log K_c$ for each individual cell holds as the single-cell case. However, we note that with the exact SINR distributions in Lemma 3.2, a more rigorous proof can be obtained, as given in the following proposition.

Proposition 3.1: For fixed M_c's and P_T, $c = 1, \cdots, C$, we have $\lim_{K_c \to \infty} \frac{R_{RBF}^{(c)}}{M_c \log_2(\eta_c \log K_c)} = 1$.

Proof: Please refer to Appendix D. ■

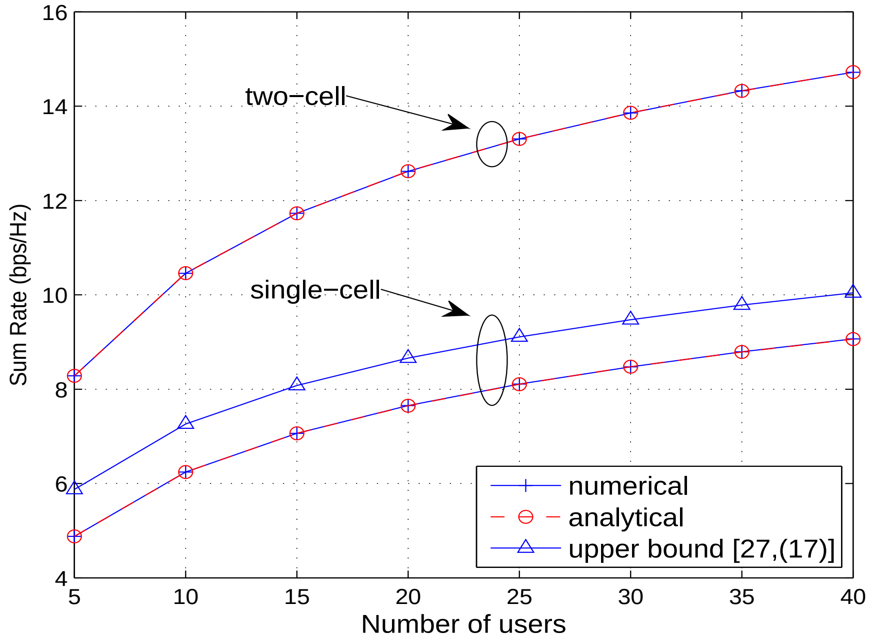

Fig. 2: Comparison of the analytical and numerical results on the RBF sum rate.

In Fig. 3, we depict both the numerical and theoretical asymptotic sum-rates for a single-cell RBF system, and the first cell of a two-cell RBF system. In the single-cell case, $\eta = 5$ dB, and $M = N_T = 3$, while in the two-cell case, $M_1 = M_2 = N_T = 3$, $\eta_1 = 5$ dB, and $\mu_{2,1} = -5$ dB. We observe that the convergence to the sum-rate scaling law $M_c \log_2(\eta_c \log K_c)$ is rather slow in both cases. For example, even with K or K_c to be 10^4, the convergence is still not clearly shown. Furthermore, Proposition 3.1 implies that the sum-rate scaling law $M_c \log_2(\eta_c \log K_c)$ holds for any cell regardless of the ICI as $K_c \to \infty$. As a consequence, this result implies that each BS should apply the maximum number of transmit beams, i.e., $M_c = N_T, \forall c$, to maximize the per-cell throughput. Such a conclusion may be misleading in a practical multi-cell system with non-negligible ICI. The above two main drawbacks, namely, slow convergence and misleading interpretation, have limited the usefulness of the conventional sum-rate scaling law $M_c \log_2(\eta_c \log K_c)$ for the multi-cell RBF. As will be shown in the next section, the DoF region approach is able to more precisely characterize the ICI effect on the throughput of the multi-cell RBF.

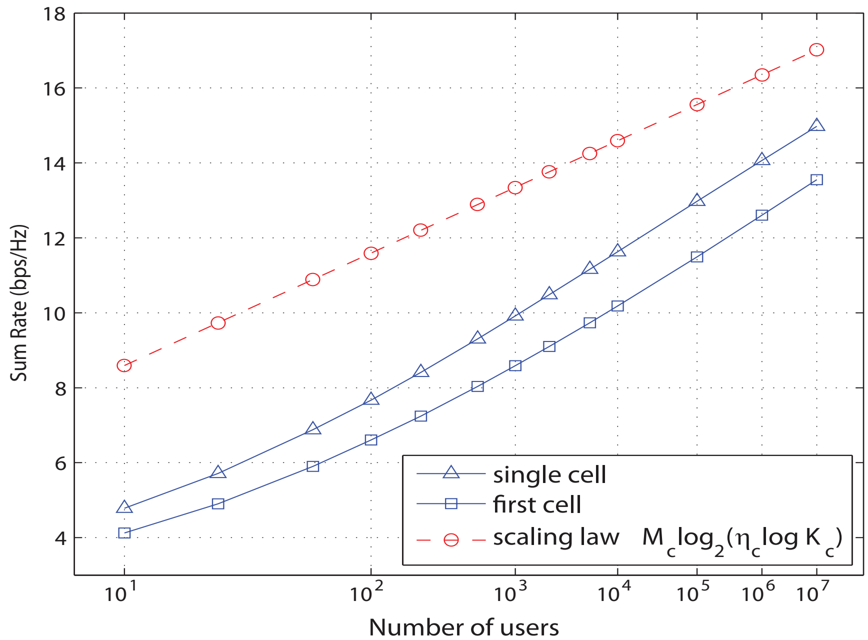

Fig. 3: Comparison of the numerical sum rate and the sum-rate scaling law for RBF.

IV. Degrees of freedom region in multi-cell Random Beamforming: high-SNR analysis

In this section, we investigate the performance of the multi-cell RBF in the high-SNR regime, i.e., when the per-cell SNR $\rho \to \infty$. In particular, we consider the approach of the DoF region, which has been defined in [10], [11], and is restated below for convenience.

Definition 4.1: (General DoF region) The DoF region of a C-cell downlink system is defined as

$$\mathcal{D} = \left\{ (d_1, d_2, \cdots, d_C) \in \mathbb{R}_+^C : \forall (\omega_1, \omega_2, \cdots, \omega_C) \in \mathbb{R}_+^C; \quad \sum_{c=1}^{C} \omega_c d_c \le \lim_{\rho \to \infty} \sup_{\boldsymbol{R} \in \mathcal{R}} \sum_{c=1}^{C} \omega_c \frac{R_{sum}^{(c)}}{\log_2 \rho} \right\}, \tag{16}$$

where ρ is the per-cell SNR; ω_c, d_c, and $R_{sum}^{(c)}$ are the non-negative rate weight, the achievable DoF, and the sum rate of the c-th cell, respectively; and the region $\mathcal{R}$ is the set of all the achievable sum-rate tuples for all the cells, denoted by $\boldsymbol{R} = (R_{sum}^{(1)}, R_{sum}^{(2)}, \cdots, R_{sum}^{(C)})$.

If the multi-cell RBF is deployed, the achievable DoF region defined in (16) is reduced to

Definition 4.2: (DoF region with RBF) The DoF region of a C-cell RBF system is given by

$$\mathcal{D}_{RBF} = \left\{ (d_1, d_2, \cdots, d_C) \in \mathbb{R}_+^C : \forall (\omega_1, \omega_2, \cdots, \omega_C) \in \mathbb{R}_+^C; \quad \sum_{c=1}^{C} \omega_c d_c \le \lim_{\rho \to \infty} \max_{M_1, \ldots, M_C \in \{0, \cdots, N_T\}} \sum_{c=1}^{C} \omega_c \frac{R_{\text{RBF}}^{(c)}}{\log_2 \rho} \right\}. \tag{17}$$

Certainly, $\mathcal{D}_{RBF} \subseteq \mathcal{D}$. Note that the DoF region is, in general, applicable for any number of users per cell, K_c. However, if it is assumed that all K_c's are constant with $\rho \to \infty$, it can be shown that the DoF region for the multi-cell RBF given in (17) will collapse to the null point, i.e., a zero DoF for all the cells, due to the intra-/inter-cell interference.[2] It thus follows that for analytical tractability, the DoF region characterization for the multi-cell RBF should have K_c increase in a certain order with the SNR, ρ. We thus make the following assumption for the rest of this paper:

Assumption 4.1: The number of users in each cell scales with ρ in the order of ρ^{α_c}, with $\alpha_c \geq 0$, denoted by $K_c = \Theta(\rho^{\alpha_c}), c = 1, \ldots, C$, i.e., $K_c/\rho^{\alpha_c} \to a_c$ as $\rho \to \infty$, with a_c being a positive constant independent of α_c.

Considering the number of per-cell users to scale polynomially with the SNR is general as well as convenient. The linear scaling law, i.e., $K_c = \beta_c \rho$, with constant $\beta_c > 0$, is only a special case of $K_c = \Theta(\rho^{\alpha_c})$ with $\alpha_c = 1$; if K_c is a constant, then the corresponding α_c is zero. We can thus consider α_c as a measure of the user density in the c-th cell given the same coverage area for all the cells, where a larger α_c indicates a higher number of users, K_c. As will be shown later in this section, Assumption 4.1 enables us to obtain an efficient as well as insightful characterization of the DoF region for the multi-cell RBF. Note that the DoF region under Assumption 4.1 can be considered as a generalization of the conventional DoF region analysis based on IA [10] for the case of finite number of users, to the case of asymptotically large number of users that scales with the SNR. For the notational convenience, we use $\mathcal{D}(\boldsymbol{\alpha})$ and $\mathcal{D}_{RBF}(\boldsymbol{\alpha})$ to denote the achievable DoF regions $\mathcal{D}$ and $\mathcal{D}_{RBF}$, respectively, corresponding to $K_c = \Theta(\rho^{\alpha_c})$, $c = 1,\cdots,C$, and $\boldsymbol{\alpha} = [\alpha_1, \cdots, \alpha_C]^T$.

A. Single-Cell Case

First, we investigate the DoF for the achievable sum rate in the single-cell RBF case without the ICI. We drop the cell index c for brevity. In the single-cell case, the DoF region collapses to a line, bounded by 0 and $d^*_{RBF}(\alpha)$, where $d^*_{RBF}(\alpha) \geq 0$ denotes the maximum DoF achievable for the RBF sum rate.

We define the achievable DoF for single-cell RBF with a given pair of α and M as

$$d_{RBF}(\alpha, M) = \lim_{\rho\to\infty} \frac{R_{\text{RBF}}}{\log_2 \rho} = \lim_{\eta\to\infty} \frac{R_{\text{RBF}}}{\log_2 \eta} \tag{18}$$

since $\eta = \rho/M$. Thus, we have $d^*_{RBF}(\alpha) = \max_{M\in\{1,\cdots,N_T\}} d_{RBF}(\alpha, M)$ for a given $\alpha \geq 0$. We first characterize $d_{RBF}(\alpha, M)$ in the following lemma.

[2] A rigorous proof of this claim can be deduced from Lemma 4.2 and Theorem 4.2 later for the special case of $\alpha_c = 0$, $\forall c$, i.e., all cells having a constant number of users.

Lemma 4.1: Assuming $K = \Theta(\rho^\alpha)$, the DoF of single-cell RBF with $M \leq N_T$ orthogonal transmit beams is given by

$$d_{RBF}(\alpha, M) = \begin{cases} \dfrac{\alpha M}{M-1}, & 0 \leq \alpha \leq M-1, \quad (19a) \\ M, & \alpha > M-1. \quad (19b) \end{cases}$$

Proof: Please refer to Appendix E. ■

Remark 4.1: With RBF and under the assumption $K = \Theta(\rho^\alpha)$, it is interesting to observe from Lemma 4.1 that the achievable DoF can be a non-negative real number (as compared to the conventional integer DoF in the literature with finite K). Moreover, it is observed that for any given $0 < \alpha < N_T - 1$, assigning more transmit beams by increasing M initially improves the sum-rate DoF if $M \leq \alpha + 1$; however, as $M > \alpha + 1$, the DoF may not necessarily increase with M due to the more dominant inter-beam/intra-cell interference. Note that the term $M - 1$ in the denominator of (19a) is exactly the number of interfering beams to one particular data beam. Thus, Lemma 4.1 provides a succinct description of the interplay between the available multiuser diversity (specified by α with a larger α denoting a higher user density or the number of users in a cell), the level of the intra-cell interference (specified by $M - 1$), and the achievable spatial multiplexing gain or DoF, $d_{RBF}(\alpha, M)$.

Next, we obtain the maximum achievable DoF for a given α by searching over all possible values of M. We note that for any $M < \lfloor\alpha\rfloor + 1$, $d_{RBF}(\alpha, M) < d_{RBF}(\alpha, \lfloor\alpha\rfloor + 1)$, while for any $M > \lfloor\alpha\rfloor + 2$, $d_{RBF}(\alpha, M) < d_{RBF}(\alpha, \lfloor\alpha\rfloor + 2)$. Thus we only need to compare $d_{RBF}(\alpha, \lfloor\alpha\rfloor + 1)$ and $d_{RBF}(\alpha, \lfloor\alpha\rfloor + 2)$ in searching for the optimal M. The result is shown in the following theorem.

Theorem 4.1: For the single-cell RBF with N_T transmit antennas and user density coefficient α, the maximum achievable DoF and the corresponding optimal number of transmit beams are[3]

$$d^*_{RBF}(\alpha) = \begin{cases} \lfloor\alpha\rfloor + 1, & \alpha \leq N_T - 1, 1 \geq \{\alpha\}(\lfloor\alpha\rfloor + 2), \\ \frac{\alpha(\lfloor\alpha\rfloor+2)}{\lfloor\alpha\rfloor+1}, & \alpha \leq N_T - 1, \{\alpha\}(\lfloor\alpha\rfloor + 2) > 1, \\ N_T, & \alpha > N_T - 1. \end{cases} \quad (20)$$

$$M^*_{RBF}(\alpha) = \begin{cases} \lfloor\alpha\rfloor + 1, & \alpha \leq N_T - 1, 1 \geq \{\alpha\}(\lfloor\alpha\rfloor + 2), \\ \lfloor\alpha\rfloor + 2, & \alpha \leq N_T - 1, \{\alpha\}(\lfloor\alpha\rfloor + 2) > 1, \\ N_T, & \alpha > N_T - 1. \end{cases} \quad (21)$$

[3]The notations $\lfloor\alpha\rfloor$ and $\{\alpha\}$ denote the integer and fractional parts of a real number α, respectively.

In Fig. 4, we use simulations to confirm Lemma 4.1. It is observed that the newly obtained sum-rate scaling law, $R_{\text{RBF}} = d_{RBF}(\alpha, M)\log_2\rho$, in the single-cell RBF case is very accurate, even for small values of SNR ρ and number of users $K = \lfloor \rho^{\alpha} \rfloor$. Compared with Fig. 3 for the conventional scaling law $R_{\text{RBF}} = M\log_2(\eta\log K)$, a much quicker convergence is observed here. The DoF approach thus provides a more efficient way of characterizing the achievable sum rate for single-cell RBF. Also observe that the sum rate for $M = 2$ is higher than that for $M = 4$. This is because with $N_T = 4$ and $\alpha = 1$ in this example, the optimal number of beams to achieve $d^*_{RBF}(1) = 2$ is $M^*_{RBF}(1) = 2$ from (21). Since many previous studies have observed that adjusting the number of beams according to the number of users in single-cell RBF can improve the achievable sum rate (see, e.g., [30]-[32]), our study here can be considered as a theoretical explanation for such an observation.

In Fig. 5, we show the maximum DoF and the corresponding optimal number of transmit beams versus the user density coefficient α with $N_T = 4$ for single-cell RBF, according to Theorem 4.1. It is observed that to maximize the achievable sum rate, we should only transmit more data beams when the number of users increases beyond a certain threshold. It is also observed that the maximum DoF $d^*_{RBF}(\alpha) = 4$ with $M = N_T = 4$ is attained when $\alpha \geq 3$ since $M^*_{RBF}(3) = 4$.

B. Multi-Cell Case

In this subsection, we extend the DoF analysis for the single-cell RBF to the more general multi-cell RBF subject to the ICI. For convenience, we denote the achievable sum-rate DoF of the c-th cell as $d_{RBF,c}(\alpha_c, \boldsymbol{m}) = \lim_{\rho\to\infty} \frac{R^{(c)}_{\text{RBF}}}{\log_2\rho}$, where $\boldsymbol{m} = [M_1, \cdots, M_C]^T$ is a given set of numbers of transmit beams at different BSs. We then state the following lemma on the achieve DoF of the c-th cell.

Lemma 4.2: In the multi-cell RBF, assuming $K_c = \Theta(\rho^{\alpha_c})$, the achievable DoF of the c-th cell $d_{RBF,c}(\alpha_c, \boldsymbol{m})$, $c \in \{1, \ldots, C\}$, for a given $\boldsymbol{m}$ is

$$d_{RBF,c}(\alpha_c, \boldsymbol{m}) = \begin{cases} \dfrac{\alpha_c M_c}{\sum_{l=1}^{C} M_l - 1}, & 0 \leq \alpha_c \leq \sum_{l=1}^{C} M_l - 1, \quad \text{(22a)} \\ M_c, & \alpha_c > \sum_{l=1}^{C} M_l - 1. \quad \text{(22b)} \end{cases}$$

Proof: The proof uses Lemma 3.2 and similar arguments in the proof of Lemma 4.1, and is thus omitted for brevity. ■

Remark 4.2: Similar to Lemma 4.1 for the single-cell case, Lemma 4.2 reveals the relationship among the multi-user diversity, the level of the interference, and the achievable DoF for multi-cell RBF. However, as compared to the single-cell case, there are not only $M_c - 1$ intra-cell interfering beams, but also

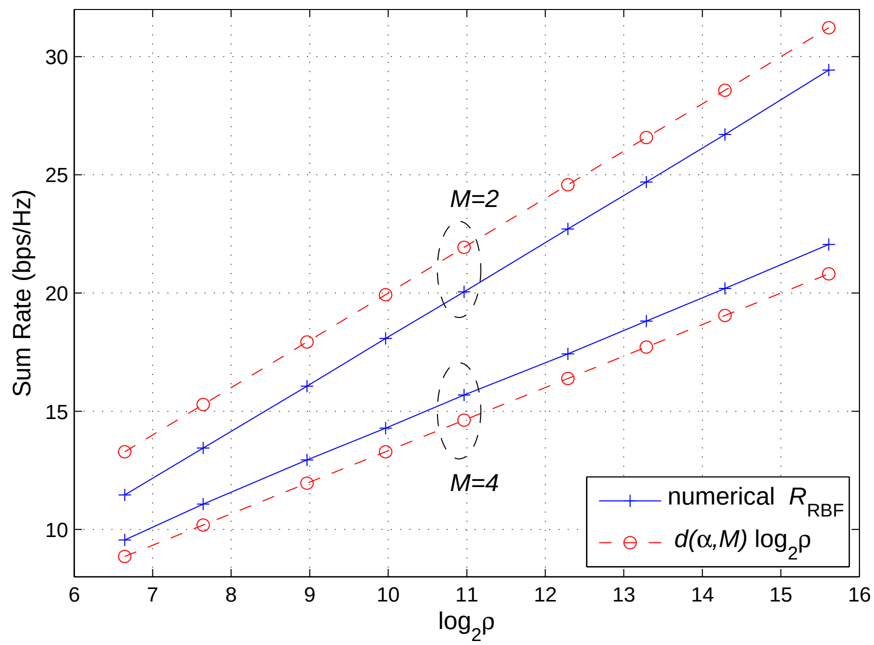

Fig. 4: Comparison of the numerical sum rate and the scaling law $d_{RBF}(\alpha, M)\log_2\rho$, with $N_T = 4$, $\alpha = 1$, and $K = \lfloor \rho^\alpha \rfloor$.

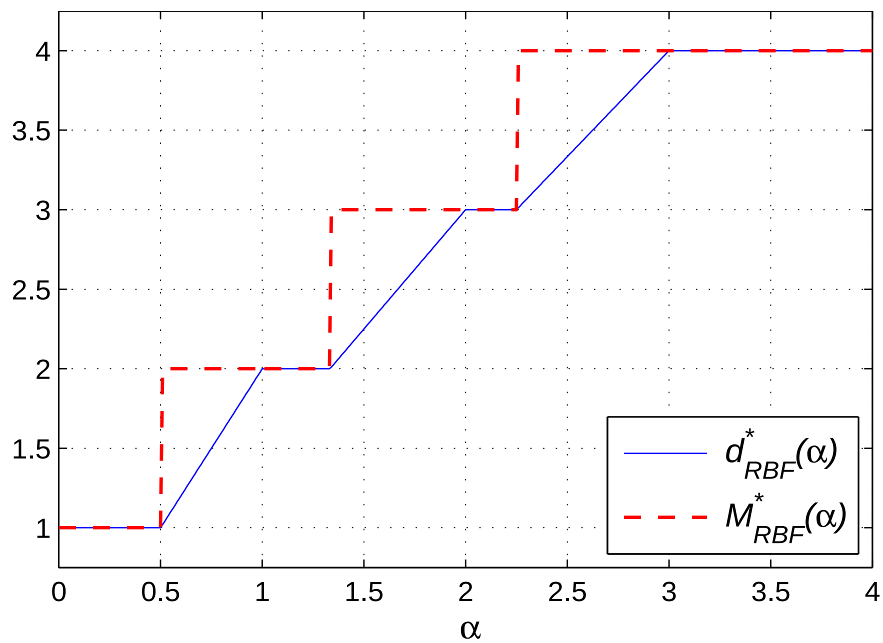

Fig. 5: The maximum DoF $d^*_{RBF}(\alpha)$ and optimal number of beams $M^*_{RBF}(\alpha)$ with $N_T = 4$.

$\sum_{l=1,l\neq c}^{C} M_l$ inter-cell interfering beams for any data beam of the c-th cell in the multi-cell case, as observed from the denominator in (22a), which results in a decrease of the achievable DoF per cell.

Next, we obtain characterization of the DoF region defined in (17) for the multi-cell RBF with any given set of per-cell user density coefficients, denoted by $\boldsymbol{\alpha} = [\alpha_1, \cdots, \alpha_C]^T$ in the following theorem; for convenience, we denote $\boldsymbol{d}_{RBF}(\boldsymbol{\alpha}, \boldsymbol{m}) = \left[\, d_{RBF,1}(\alpha_1, \boldsymbol{m}) \,, \cdots, \, d_{RBF,C}(\alpha_C, \boldsymbol{m})\right]^T$, with $d_{RBF,c}(\alpha_c, \boldsymbol{m})$ given in Lemma 4.2.

Theorem 4.2: Assuming $K_c = \Theta\left(\rho^{\alpha_c}\right), c = 1, \ldots, C$, the achievable DoF region of a C-cell RBF system is given by

$$\mathcal{D}_{RBF}(\boldsymbol{\alpha}) = \boldsymbol{conv}\Big\{\boldsymbol{d}_{RBF}(\boldsymbol{\alpha}, \boldsymbol{m}), M_c \in \{0, \cdots, N_T\}, \; c = 1, \cdots, C\Big\}, \tag{23}$$

where $\boldsymbol{conv}$ denotes the convex hull operation.

Theorem 4.2 is obtained directly using Lemma 4.2 and the definition of the DoF region, for which the proof is omitted for brevity. This theorem implies that we can obtain the DoF region of multi-cell RBF $\mathcal{D}_{RBF}(\boldsymbol{\alpha})$ by taking the convex hull over all achievable DoF points $\boldsymbol{d}_{RBF}(\boldsymbol{\alpha}, \boldsymbol{m})$ with all different values of $\boldsymbol{m}$, i.e., different BS beam number assignments.

In Fig. 6, we depict the DoF region of a two-cell RBF system with $N_T = 4$, and for different user density coefficients α_1 and α_2. The vertices of these regions can be obtained by setting appropriate numbers of beams $0 \leq M_1 \leq 4$ and $0 \leq M_2 \leq 4$, while time-sharing between these vertices yields the entire boundary. To achieve the maximum sum-DoF of both cells, it is observed that a rule of thumb is to transmit more beams in the cell with a higher user density, and when α_1 and α_2 are both small, even turn off the BS of the cell with the smaller user density. Since the maximum sum-DoF does not consider the throughput fairness, the DoF region clearly shows all the achievable sum-rate tradeoffs among different cells, by observing its (Pareto) boundary as shown in Fig. 6. It is also observed that switching the two BSs to be on/off alternately achieves the optimal DoF boundary when the numbers of users in both cells are small, but is strictly suboptimal when the user number becomes large (see the dashed line in Fig. 6).

Furthermore, consider the case without any cooperation between these two BSs in assigning their numbers of transmit beams, i.e., both cells act selfishly by transmitting $M_c = N_T$ beams to aim to maximize their own DoF. The resulting DoF pairs, denoted by $\boldsymbol{d}_{RBF}([\alpha_1, \alpha_2], [4, 4])$, for three sets of $\boldsymbol{\alpha}$ are shown in Fig. 6 as P_1, P_2, and P_3, respectively. It is observed that the smaller the user densities are, the further the above non-cooperative multi-cell RBF scheme deviates from the Pareto boundary. In general, the optimal DoF tradeoffs or the boundary DoF pairs are achieved when both cells cooperatively assign their numbers of transmit beams based on their respective user densities, especially when the

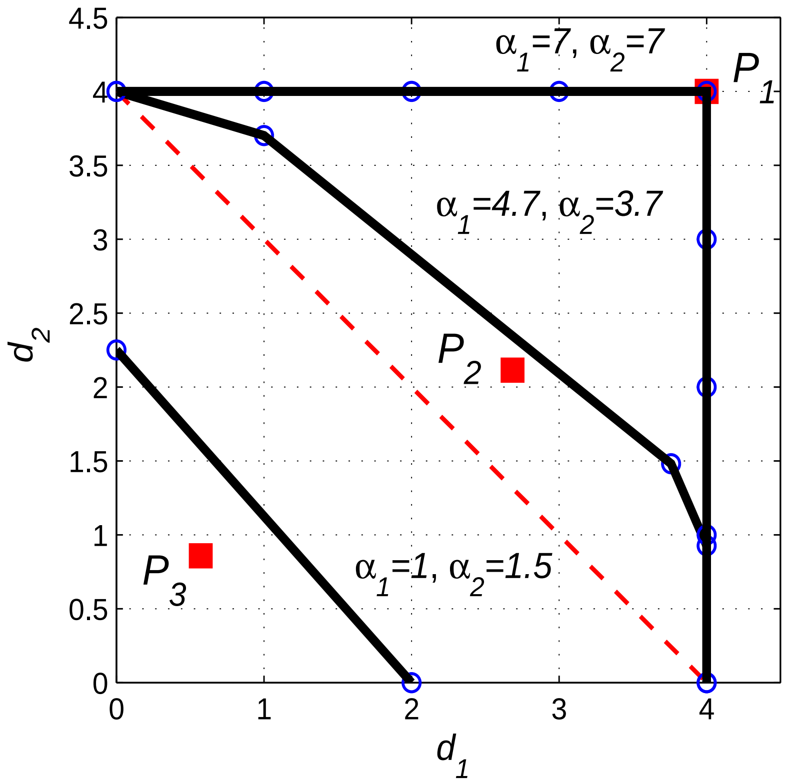

Fig. 6: DoF region of two-cell RBF system with $N_T = 4$.

numbers of users in both cells are not sufficiently large. Since the information needed to determine the optimal operating DoF point is only the individual cell user density coefficients, the DoF region provides a very useful method to globally optimize the coordinated multi-cell RBF scheme in practical systems.

C. Optimality of Multi-Cell RBF

So far, we have characterized the achievable DoF region for the multi-cell RBF scheme that requires only partial CSI at the transmitter. One important question that remains unaddressed yet is how the multi-cell RBF performs as compared to the optimal transmission scheme (e.g., IA) for the multi-cell downlink system with the full transmitter CSI, in terms of achievable DoF region. In this subsection, we attempt to partially answer this question by focusing on the regime given in Assumption 4.1, i.e., the number of users per cell scales with a polynomial order with the SNR as the SNR goes to infinity.

1) Single-Cell Case: First, we consider the single-cell case to draw some useful insights. It is well known that the maximum sum-rate DoF for a single-cell MISO-BC with N_T transmit antennas and $K \geq N_T$ single-antenna users with independent channels is N_T [2], which is achievable by the DPC scheme or even simple linear precoding schemes. However, it is not immediately clear whether such a

result still holds for the case of $K = \Theta(\rho^{\alpha}) \gg N_T$ with $\alpha > 0$, since in this case N_T may be only a lower bound on the maximum DoF. We thus have the following proposition.

Proposition 4.1: Assuming $K = \Theta(\rho^{\alpha})$ with $\alpha > 0$, the maximum sum-rate DoF of a single-cell MISO-BC with N_T transmit antennas is $d^*(\alpha) = N_T$.

Proof: Please refer to Appendix F. ■

Proposition 4.1 confirms that the maximum DoF of the MISO-BC is still N_T, even with the asymptotically large number of users that scales with SNR, i.e., multiuser diversity does not yield any increment of DoF. Since from Section IV-A, we know that the DoF region for the single-cell RBF scheme is a line, which is bounded by 0 and $d^*_{RBF}(\alpha)$, where $d^*_{RBF}(\alpha)$ is specified in Theorem 4.1. In addition, for $\alpha \geq N_T - 1$, $d^*_{RBF}(\alpha) = N_T$. We thus have the following proposition.

Proposition 4.2: Assuming $K = \Theta(\rho^{\alpha})$, the single-cell RBF scheme is DoF-optimal if $\alpha \geq N_T - 1$.

From the above proposition, it follows that the single-cell RBF achieves the maximum DoF with $M = N_T$ if the number of users is sufficiently large, thanks to the multiuser diversity effect that completely eliminates the intra-cell interference given a sufficiently large number of users.

2) Multi-Cell Case: For the convenience of analysis, we use $\mathcal{D}_{\mathrm{UB}}(\boldsymbol{\alpha})$ to denote an upper bound on the DoF region defined in (16), for a given $\boldsymbol{\alpha}$ in the multi-cell case. Clearly, under Assumption 4.1, it follows that $\mathcal{D}_{RBF}(\boldsymbol{\alpha}) \subseteq \mathcal{D}(\boldsymbol{\alpha}) \subseteq \mathcal{D}_{\mathrm{UB}}(\boldsymbol{\alpha})$.

The following proposition establishes the DoF region upper bound $\mathcal{D}_{\mathrm{UB}}(\boldsymbol{\alpha})$.

Proposition 4.3: Given $K_c = \Theta(\rho^{\alpha_c})$, $c = 1, \cdots, C$, a DoF region upper bound for a C-cell MISO downlink system is given by

$$\mathcal{D}_{\mathrm{UB}}(\boldsymbol{\alpha}) = \left\{ (d_1, d_2, \cdots d_C) \in \mathbb{R}_+^C : d_c \leq N_T, c = 1, \cdots, C \right\}. \tag{24}$$

The above proposition can be easily shown by noting that $d_c \leq N_T$ is a direct consequence of Proposition 4.1 for the single-cell case, which should also hold for the multi-cell case by ignoring the ICI in each of the cells, i.e., an ICI-free multi-cell downlink system is considered. Supposing $\alpha_c \geq CN_T - 1$, c = 1, $\cdots$, C, from Lemma 4.2 and Theorem 4.2, it easily follows that the achievable DoF region of multi-cell RBF in this case is $\mathcal{D}_{RBF}(\boldsymbol{\alpha}) = \mathcal{D}_{\mathrm{UB}}(\boldsymbol{\alpha})$. This leads to $\mathcal{D}_{RBF}(\boldsymbol{\alpha}) \subseteq \mathcal{D}(\boldsymbol{\alpha}) \subseteq \mathcal{D}_{\mathrm{UB}}(\boldsymbol{\alpha}) = \mathcal{D}_{RBF}(\boldsymbol{\alpha})$, and thus $\mathcal{D}_{RBF}(\boldsymbol{\alpha}) = \mathcal{D}(\boldsymbol{\alpha})$, i.e., the multi-cell RBF achieves the exact DoF region in this regime. We thus have the following proposition.

Proposition 4.4: Given $K_c = \Theta(\rho^{\alpha_c})$, $c = 1, \cdots, C$, the multi-cell RBF scheme achieves the DoF region of a C-cell MISO downlink system, i.e., $\mathcal{D}_{RBF}(\boldsymbol{\alpha}) = \mathcal{D}(\boldsymbol{\alpha})$, if $\alpha_c \geq CN_T - 1$, $\forall c \in \{1, \cdots, C\}$.

Remark 4.3: The above proposition implies that the multi-cell RBF is indeed DoF-optimal when the numbers of users in all cells are sufficiently large. Due to the overwhelming multiuser diversity gain, RBF compensates the lack of full CSI at transmitters without any compromise of DoF degradation. However, it is important to point out that such a result should not undermine the benefits of having the more complete CSI at transmitters in practical multi-cell systems, where more sophisticated precoding schemes than RBF such as IA-based ones [10] can be applied to achieve substantial throughput gains, especially when the numbers of per-cell users are not so large. Due to the space limitation, we do not make a detailed comparison of the achievable rates between IA and RBF for the case of finite number of users in this paper, and will leave this interesting study in our further work.

V. Conclusions

In this paper, the achievable rates of the RBF scheme in a multi-cell setup subject to the ICI are thoroughly investigated. Both finite-SNR and high-SNR regimes are considered. For the finite-SNR case, we provide closed-form expressions of the achievable average sum rates for both single- and multi-cell RBF with a finite number of users per cell. We also derive the sum-rate scaling law in the conventional asymptotic regime, i.e., when the number of users goes to infinity with a fixed SNR. Since the finite-SNR analysis has major limitations, we furthermore consider the high-SNR regime by adopting the DoF-region approach to characterize the optimal throughput tradeoffs among different cells in multi-cell RBF, assuming that the number of users per cell scales in a polynomial order with the SNR when the SNR goes to infinity. We show the closed-form expressions of the achievable DoF and the corresponding optimal number of transmit beams, both as functions of the user number scaling order or the user density, for the single-cell case. From this result, we obtain a complete characterization of the DoF region for the multi-cell RBF, in which the optimal boundary DoF point is achieved by BSs' cooperative assignment of their numbers of transmit beams according to individual user densities. Finally, if the numbers of users in all cells are sufficiently large, we show that the multi-cell RBF, albeit requiring only partial CSI at transmitters, achieve the optimal DoF region even with the full transmit CSI. The results of this paper are useful for the optimal design of multi-cell RBF in practical cellular systems with limited channel feedback.

Appendix A
Proof of Lemma 3.1

It is easy to see that

$$\mathbb{E}\left[\log_2\left(1+\max_{k\in\{1,\cdots,K\}}\mathrm{SINR}_{k,1}\right)\right]=\int_0^\infty \log_2(1+x)Kf_S(x)F_S^{K-1}(x)dx, \tag{25}$$

where $f_S(s)$ and $F_S(s)$ are given in (7) and (8). Therefore, the RBF sum rate can be obtained as follows.

$$\begin{aligned}
R_{\mathrm{RBF}} &= M\int_0^\infty \log_2(1+x)Kf_S(x)F_S^{K-1}(x)dx=\frac{M}{\log 2}\int_0^\infty \log(1+x)d\big(F_S^K(x)\big)\\
&=\frac{M}{\log 2}F_S^K(x)\log(1+x)\Big|_0^\infty-\frac{M}{\log 2}\int_0^\infty\frac{1}{1+x}\left(1-\frac{\exp(-x/\eta)}{(1+x)^{M-1}}\right)^K dx\\
&=\frac{M}{\log 2}\lim_{x\to\infty}\big(F_S^K(x)-1\big)\log(1+x)+\frac{M}{\log 2}\sum_{n=1}^{K}(-1)^n\binom{K}{n}\int_0^\infty\frac{\exp(-nx/\eta)dx}{(1+x)^{n(M-1)+1}}\\
&=\frac{M}{\log 2}\sum_{n=1}^{K}(-1)^n\binom{K}{n}e^{-n/\eta}\int_1^\infty\frac{\exp(-ny/\eta)dy}{y^{n(M-1)+1}}.
\end{aligned} \tag{26}$$

Now by using [29, 2.324.2], (9) can be obtained. This completes the proof of Lemma 3.1.

Appendix B

Proof of Lemma 3.2

Denote $X=\left|\boldsymbol{h}_k^{(c,c)}\boldsymbol{\phi}_m^{(c)}\right|^2$, and

$$V=\sum_{i=1,i\neq m}^{M_c}\left|\boldsymbol{h}_k^{(c,c)}\boldsymbol{\phi}_i^{(c)}\right|^2+\sum_{l=1,l\neq c}^{M_l}\frac{\mu_{l,c}}{\eta_c}\sum_{i=1}^{M_l}\left|\boldsymbol{h}_k^{(l,c)}\boldsymbol{\phi}_i^{(l)}\right|^2. \tag{27}$$

We note that the terms $\left|\boldsymbol{h}_k^{(l,c)}\boldsymbol{\phi}_i^{(l)}\right|^2$, $\forall k,l,c,i$, are independent chi-square random variables with two degrees of freedom, denoted by $\chi^2(2)$. Using the characteristic function, we can express the PDF of V as follows.

$$f_V(v)=\frac{1}{2\pi}\int_{-\infty}^{\infty}\frac{e^{-j\omega v}d\omega}{(1-j\omega)^{M_c-1}\prod_{l=1,l\neq c}^{C}\left(1-j\frac{\mu_{l,c}}{\eta_c}\omega\right)^{M_l}}, \tag{28}$$

where $j=\sqrt{-1}$. Since $S=\frac{X}{1/\eta_c+V}$, the PDF of S is

$$f_S^{(c)}(s)=\int_0^\infty f_{S|V}(s|v)f_V(v)dv=A+B, \tag{29}$$

in which,

$$A=\frac{e^{-s/\eta_c}}{2\pi\eta_c}\int_{-\infty}^{\infty}\frac{d\omega}{(s+j\omega)(1-j\omega)^{M_c-1}\prod_{l=1,l\neq c}^{C}\left(1-j\frac{\mu_{l,c}}{\eta_c}\omega\right)^{M_l}}, \tag{30}$$

$$B = \frac{e^{-s/\eta_c}}{2\pi} \int_{-\infty}^{\infty} \frac{d\omega}{(s+j\omega)^2 (1-j\omega)^{M_c-1} \prod_{l=1,l\neq c}^{C} \left(1 - j\frac{\mu_{l,c}}{\eta_c}\omega\right)^{M_l}}. \tag{31}$$

We first use the partial fraction expansion to decompose A, then apply the *Cauchy integral formula* [33] to obtain

$$\begin{aligned} A &= \frac{e^{-s/\eta_c}}{2\pi\eta_c} \int_{-\infty}^{\infty} \left[\frac{A_0}{s+j\omega} + \frac{A_c}{1-j\omega} + \sum_{l=1,l\neq c}^{C} \frac{A_l}{1-j\frac{\mu_{l,c}}{\eta_c}\omega} + A'\right] d\omega \\ &= \frac{e^{-s/\eta_c}}{2\eta_c} \left(A_0 + A_c + \sum_{l=1,l\neq c}^{C} \frac{\eta_c}{\mu_{l,c}} A_l\right), \end{aligned} \tag{32}$$

where A' is the sum of all terms with order greater than 1.

Now, note that

$$\begin{aligned} 1 = {} & A_0(1-j\omega)^{M_c-1} \prod_{l=1,l\neq c}^{C} \left(1 - j\frac{\mu_{l,c}}{\eta_c}\omega\right)^{M_l} + A_c(s+j\omega)(1-j\omega)^{(M_c-2)^+} \prod_{l=1,l\neq c}^{C} \left(1 - j\frac{\mu_{l,c}}{\eta_c}\omega\right)^{M_l} \\ & + (s+j\omega)(1-j\omega)^{M_c-1} \sum_{l=1,l\neq c}^{C} \left[A_l \left(1 - j\frac{\mu_{l,c}}{\eta_c}\omega\right)^{M_l-1} \prod_{n=1,n\neq l,c}^{C} \left(1 - j\frac{\mu_{n,c}}{\eta_c}\omega\right)^{M_n}\right] \\ & + A'(s+j\omega)\,(1-j\omega)^{M_c-1} \prod_{l=1,l\neq c}^{C} \left(1 - j\frac{\mu_{l,c}}{\eta_c}\omega\right)^{M_l}. \end{aligned} \tag{33}$$

where the notation $(x)^+$ represents $\max(x,0)$. Substituting $\omega = -s/j$, we have

$$A_0 = \frac{1}{(1+s)^{M_c-1} \prod_{l=1,l\neq c}^{C} (1 + \frac{\mu_{l,c}}{\eta_c}s)^{M_l}}. \tag{34}$$

Also, by observing the coefficient of $\omega^{(\sum_{l=1}^{C} M_l - 1)}$, (33) leads to $A_0 = A_c + \sum_{l=1,l\neq c}^{C} \frac{\eta_c}{\mu_{l,c}} A_l$. Therefore, from (32), we conclude

$$A = \frac{e^{-s/\eta_c}}{\eta_c} A_0 = \frac{e^{-s/\eta_c}}{\eta_c (1+s)^{M_c-1} \prod_{l=1,l\neq c}^{C} (1 + \frac{\mu_{l,c}}{\eta_c}s)^{M_l}}. \tag{35}$$

By differentiating A in (32) with respect to s, we obtain $\frac{dA}{ds} = -\frac{A}{\eta_c} - \frac{B}{\eta_c}$, i.e., $f_S^{(c)}(s) = A + B = -\eta_c \frac{dA}{ds}$. Combining this result and (35), (10) and (11) are obtained. This completes the proof of Lemma 3.2.

Appendix C
Proof of Theorem 3.1

Using the similar derivation as in Appendix A, we obtain

$$
\begin{aligned}
R_{\text{RBF}}^{(c)} &= \frac{M_c}{\log 2}\sum_{n=1}^{K_c}(-1)^n\binom{K_c}{n}\int_0^\infty \frac{\exp(-nx/\eta)dx}{(1+x)^{n(M_c-1)+1}\prod_{l=1,l\neq c}^{C}\left(\frac{\mu_{l,c}}{\eta_c}x+1\right)^{nM_l}} \\
&= \frac{M_c}{\log 2}\sum_{n=1}^{K_c}(-1)^n\binom{K_c}{n}\prod_{l=1,l\neq c}^{C}\left(\frac{\eta_c}{\mu_l}\right)^{nM_l}\int_0^\infty \frac{\exp(-nx/\eta)dx}{(x+1)^{n(M_c-1)+1}\prod_{l=1,l\neq c}^{C}\left(x+\frac{\eta_c}{\mu_{l,c}}\right)^{nM_l}}.
\end{aligned}
\tag{36}
$$

By applying the partial fractional decomposition given in (13) and using [29, 2.234.2] for each term therein, we arrive at (12). This completes the proof of Theorem 3.1.

Appendix D
Proof of Proposition 3.1

Due to the similarity between (8) and (11), the original approach in [7, Theorem 1] can be applied to prove this proposition with minor modifications. For the completeness, only a sketch proof is presented here.

To show that $R_{\text{RBF}}^{(c)} \xrightarrow{K_c\to\infty} M_c\log_2\log K_c$, we first note that $f_S^{(c)}(s)$ and $F_S^{(c)}(s)$ satisfies the *von Mises condition* for the Gumbel-type limiting distributions (see, e.g., [34, Theorem 10.5.2.c]). Therefore, as $K_c\to\infty$, there exist constants a_{K_c} and b_{K_c} such that $\left[F_S^{(c)}(a_{K_c}x+b_{K_c})\right]^{K_c}\to\exp\left(-e^{-x}\right)$. The value of b_{K_c} can be found to be[4]

$$
b_{K_c} = \eta_c\log K_c - \eta_c\left(\sum_{l=1}^{C}M_l-1\right)\log\log K_c + O(\log\log\log K_c). \tag{37}
$$

Furthermore, the growth function, defined as $g_S^{(c)}(s)=\left(1-F_S^{(c)}(s)\right)/f_S^{(c)}(s)$ for $s\geq 0$, is given by

$$
g_S^{(c)}(s) = \frac{1}{\frac{1}{\eta_c}+\frac{M_c-1}{s+1}+\sum_{l=1,l\neq c}^{C}\frac{M_l}{s+\frac{\eta_c}{\mu_{l,c}}}}. \tag{38}
$$

It is easy to verify the followings:

- $\lim_{s\to\infty} g_S^{(c)}(s)=\eta_c>0$,
- $b_{K_c}=O(\log K_c)$ as $K_c\to\infty$, and
- The derivative of $g_S^{(c)}(s)$ satisfies

$$
\left.\frac{d^n g_S^{(c)}(s)}{ds^n}\right|_{s=b_{K_c}} = O\left(\frac{1}{b_{K_c}^{n+1}}\right). \tag{39}
$$

[4]Let $f(K_c)$ be a function of K_c. $f(K_c)=O(\log\log\log K_c)$ means that $f(K_c)/\log\log\log K_c<\infty$ as $K_c\to\infty$.

Hence, by applying [7, Corollary A.1], we have

$$\Pr\left\{\eta_c \log K_c - \eta_c \left(\sum_{l=1}^{C} M_l\right) \log\log K_c + O(\log\log\log K_c) \leq \max_{k\in\{1,\cdots,K_c\}} \text{SINR}_{k,m}^{(c)} \right.$$
$$\left. \leq \eta_c \log K_c - \eta_c \left(\sum_{l=1}^{C} M_l - 2\right) \log\log K_c + O(\log\log\log K_c)\right\} \geq 1 - O\left(\frac{1}{\log K_c}\right). \quad (40)$$

This completes the proof of Proposition 3.1.

Appendix E

Proof of Lemma 4.1

For convenience, we denote the following auxiliary random variable $R_{k,m} = \log_2\left(1 + \text{SINR}_{k,m}\right)$. From (8), the CDF of $R_{k,m}$ is obtained as

$$F_R(r) = 1 - \frac{e^{-(2^r-1)/\eta}}{2^{r(M-1)}}.$$

To prove Lemma 4.1, we first show that

$$\Pr\left\{\frac{\alpha}{M-1}\log_2\eta + \log_2\log\eta \geq \max_{k\in\{1,\cdots,K\}} R_{k,1} \geq \frac{\alpha}{M-1}\log_2\eta - \log_2\log\eta\right\} \xrightarrow{\eta\to\infty} 1, \text{ if } 0 < \alpha \leq M-1, \quad (41)$$

$$\Pr\left\{\log_2\eta + \log_2\log\eta + \log_2\alpha \geq \max_{k\in\{1,\cdots,K\}} R_{k,1} \geq \log_2\eta + \log_2\log\eta + \log_2\beta\right\} \xrightarrow{\eta\to\infty} 1, \text{ if } \alpha > M-1, \quad (42)$$

in which the constant β is define as $\beta = \frac{\alpha-M+1}{2}$; hence $\alpha > \beta > 0$ when $\alpha > M-1$. Considering (41), the upper-bound probability can be expressed as

$$\Pr\left\{\frac{\alpha}{M-1}\log_2\eta + \log_2\log\eta \geq \max_{k\in\{1,\cdots,K\}} R_{k,1}\right\} = \left[F_R\left(\frac{\alpha}{M-1}\log_2\eta + \log_2\log\eta\right)\right]^K$$
$$= \left(1 - \frac{\exp\left(-\eta^{\frac{\alpha}{M-1}-1}\log\eta\right)\exp\left(\eta^{-1}\right)}{\eta^{\alpha}(\log\eta)^{M-1}}\right)^K. \quad (43)$$

Using the asymptotic relation $\log(1-x) = -x + O(x^2)$ when x is small, we get

$$K\log\left(1 - \frac{\exp\left(-\eta^{\frac{\alpha}{M-1}-1}\log\eta\right)\exp\left(\eta^{-1}\right)}{\eta^{\alpha}(\log\eta)^{M-1}}\right) = -\frac{K}{\eta^{\alpha}(\log\eta)^{M-1}}\exp\left(-\eta^{\frac{\alpha}{M-1}-1}\log\eta\right)\exp\left(\eta^{-1}\right)$$
$$+ O\left(\frac{K}{\eta^{2\alpha}(\log\eta)^{2(M-1)}}\exp\left(-2\eta^{\frac{\alpha}{M-1}-1}\log\eta\right)\exp\left(2\eta^{-1}\right)\right) \xrightarrow{\eta\to\infty} 0, \quad (44)$$

in which we have used the assumptions $K = \Theta(\eta^{\alpha})$, and $0 < \alpha \leq M-1$. As a consequence, the upper-bound probability converges to 1 when $\eta \to \infty$. To show the convergence of the lower-bound probability in (41), we can utilize the same technique described above by showing

$$\begin{aligned} \Pr\left\{\frac{\alpha}{M-1}\log_2\eta - \log_2\log\eta \geq \max_{k\in\{1,\cdots,K\}} R_{k,1}\right\} &= \left[F_R\left(\frac{\alpha}{M-1}\log_2\eta - \log_2\log\eta\right)\right]^K \\ &= \left(1 - \frac{\exp\left(-\frac{1}{\log\eta}\eta^{\frac{\alpha}{M-1}-1}\right)\exp\left(\eta^{-1}\right)(\log\eta)^{M-1}}{\eta^{\alpha}}\right)^K. \end{aligned} \tag{45}$$

Note that

$$\begin{aligned} &K\log\left(1 - \frac{\exp\left(-\frac{1}{\log\eta}\eta^{\frac{\alpha}{M-1}-1}\right)\exp\left(\eta^{-1}\right)(\log\eta)^{M-1}}{\eta^{\alpha}}\right) \\ &= -\frac{K}{\eta^{\alpha}}(\log\eta)^{M-1}\exp\left(-\frac{1}{\log\eta}\eta^{\frac{\alpha}{M-1}-1}\right)\exp\left(\eta^{-1}\right) \\ &\quad + O\left(\frac{K}{\eta^{2\alpha}}(\log\eta)^{2(M-1)}\exp\left(-\frac{2}{\log\eta}\eta^{\frac{\alpha}{M-1}-1}\right)\exp\left(2\eta^{-1}\right)\right) \xrightarrow{\eta\to\infty} -\infty, \end{aligned} \tag{46}$$

since, when $\eta \to \infty$, the first term in (46) goes to $-\infty$, while the second term goes to 0. (45) thus converges to 0 and the lower-bound probability is confirmed. The proof of (42) follows similar arguments as the above, and is omitted for brevity. This completes the proof of Lemma 4.1.

Appendix F
Proof of Proposition 4.1

According to the main text, it is sufficient to show the DoF upper bound to be N_T as follows. Note that in a single-cell MISO-BC, the DPC yields the optimal sum rate, denoted by R_{DPC}. Therefore, $d^*(\alpha) = \lim_{\rho\to\infty}\frac{R_{\text{DPC}}}{\log_2\rho}$. From [35, Theorem 1], we have

$$R_{\text{DPC}} \leq N_T\mathbb{E}\left[\log_2\left[1 + \eta\max_{k\in\{1,\cdots,K\}}||\boldsymbol{h}_k||^2\right]\right]. \tag{47}$$

Note that $\eta = P_T/(N_T\sigma^2)$ is the SNR per beam, and $||\boldsymbol{h}_k||^2$'s are i.i.d. chi-square random variables with $2N_T$ degrees of freedom, denoted by $\chi^2(2N_T)$. Thus, if we denote $R_k = \log_2(1+\eta||\boldsymbol{h}_k||^2)$, the CDF of $R = R_k$ is $F_R(r) = \frac{1}{\Gamma(N_T)}\gamma\left(N_T, \frac{2^r-1}{\eta}\right)$, where $\Gamma(\cdot)$ and $\gamma(\cdot,\cdot)$ are the gamma and the incomplete gamma function, respectively. The same reasoning as in the proof of Lemma 4.1 can be reused here to show that

$$\Pr\left\{\log_2\eta + \log_2\log\eta + \log_2(\alpha+1) \geq \max_{k\in\{1,\cdots,K\}} R_k\right\} \xrightarrow{\eta\to\infty} 1. \tag{48}$$

This completes the proof of Proposition 4.1.

REFERENCES

[1] M. Costa, “Writing on dirty paper,” *IEEE Trans. Inf. Theory*, vol. 29, no. 3, pp. 439-441, May 1983.

[2] G. Caire and S. Shamai, “On the achievable throughput of a multi-antenna Gaussian broadcast channel,” *IEEE Trans. Inf. Theory*, vol. 49, pp. 1691-1706, July 2003.

[3] H. Weingarten, Y. Steinberg, and S. Shamai, “The capacity region of the Gaussian multiple-input multiple-output broadcast channel,” *IEEE Trans. Inf. Theory*, vol. 52, No. 9, pp. 3936-3964, Sep. 2006.

[4] Q. H. Spencer, A. L. Swindlehurst, and M. Haardt, “Zero-forcing methods for downlink spatial multiplexing in multiuser MIMO channels,” *IEEE Trans. Signal Process.*, vol. 52, no. 2, pp. 461-471, Feb. 2004.

[5] N. Jindal, “MIMO broadcast channels with finite-rate feedback,” *IEEE Trans. Inf. Theory*, vol. 52, pp. 5045-5060, Nov. 2006.

[6] P. Viswanath, D. N. C. Tse, and R. Laroia, “Opportunistic beamforming using dumb antennas,” *IEEE Trans. Inf. Theory*, vol. 48, no. 6, pp. 1277-1294, June 2002.

[7] M. Sharif and B. Hassibi, “On the capacity of MIMO broadcast channel with partial side information,” *IEEE Trans. Inf. Theory*, vol. 51, no. 2, pp. 506-522, Feb. 2005.

[8] M. Sharif and B. Hassibi, “A comparison of time-sharing, beamforming, and DPC for MIMO broadcast channels with many users,” *IEEE Trans. Commun.*, vol. 55, no. 2, pp. 11-15, Jan. 2007.

[9] S.-H. Moon, S.-R. Lee, and I. Lee, “Sum-rate capacity of random beamforming for multi-antenna broadcast channels with other cell interference,” *IEEE Trans. Wireless Commun.*, vol. 10, no. 8, pp. 2440-2444, Aug. 2011.

[10] S. A. Jafar, “Interference alignment: a new look at signal dimensions in a communication network”, *Foundations and Trends in Communications and Information Theory*, vol. 7, no. 1, pp 1-136, 2011.

[11] T. Gou and S. A. Jafar, “Degrees of freedom of the K user $M \times N$ MIMO interference channel,” *IEEE Trans. Inf. Theory*, vol. 56, no. 12, pp. 6040-6057, Dec. 2010.

[12] V. R. Cadambe and S. A. Jafar, “Interference alignment and degrees of freedom of the K-user interference channel,” *IEEE Trans. Inf. Theory*, vol. 54, pp. 3425-3441, Aug. 2008.

[13] S.-H. Park and I. Lee, “Degrees of freedom of multiple broadcast channels in the presence of inter-cell interference,” *IEEE Trans. Commun.*, vol. 59, no. 5, pp. 1481-1487, May 2011.

[14] R. Etkin, D. Tse, and H. Wang, “Gaussian interference channel capacity to within one bit,” *IEEE Trans. Inf. Theory*, vol. 54, no. 12, pp. 5534-5562, Dec. 2008.

[15] R. Zhang, “Cooperative multi-cell block diagonalization with per-base-station power constraints,” *IEEE J. Sel. Areas Commun.*, vol. 28, no. 9, pp. 1435-1445, Dec. 2010.

[16] B. Ng, J. Evans, S. Hanly, and D. Aktas, “Distributed downlink beamforming with cooperative base stations,” *IEEE Trans. Inf. Theory*, vol. 54, no. 12, pp. 5491-5499, Dec. 2008.

[17] L. Zhang, R. Zhang, Y. C. Liang, Y. Xin, and H. V. Poor, “On the Gaussian MIMO BC-MAC duality with multiple transmit covariance constraints,” *IEEE Trans. Inf. Theory*, vol. 58, no. 34, pp. 2064-2078, Apr. 2012.

[18] H. Dahrouj and W. Yu, “Coordinated beamforming for the multicell multi-antenna wireless systems,” *IEEE Trans. Wireless Commun.*, vol. 9, no. 5, pp. 1748-1795, May 2010.

[19] J. Qiu, R. Zhang, Z.-Q. Luo, and S. Cui, “Optimal distributed beamforming for MISO interference channels,” *IEEE Trans. Signal Process.*, vol. 59, no. 11 pp. 5638-5643, Nov. 2011.

[20] Y.-F. Liu, Y.-H. Dai, and Z.-Q. Luo, “Coordinated beamforming for MISO interference channel: complexity analysis and efficient algorithms,” *IEEE Trans. Signal Process.*, vol. 59, no. 3, pp. 1142-1157, Mar. 2011.

[21] X. Shang, B. Chen, and H. V. Poor, “Multiuser MISO interference channels with single-user detection: optimality of beamforming and the achievable rate region,” *IEEE Trans. Inf. Theory*, vol. 57, no. 7, pp. 4255-4273, July 2011.

[22] E. Bjornson, R. Zakhour, D. Gesbert, and B. Ottersten, “Cooperative multicell precoding: rate region characterization and distributed strategies with instantaneous and statistical CSI,” *IEEE Trans. Signal Process.*, vol. 58, no. 8, pp. 4298-4310, Aug. 2010.

[23] R. Zhang and S. Cui, “Cooperative interference management with MISO beamforming,” *IEEE Trans. Signal Process.*, vol. 58, no. 10, pp. 5450-545, Oct. 2010.

[24] H. Huh, G. Caire, S.-H. Moon, Y.-T. Kim, and I. Lee, “Multi-cell MIMO downlink with cell cooperation and fair scheduling: a large-system limit analysis,” *IEEE Trans. Inf. Theory*, vol. 57, no. 12, pp. 7771-7786, Dec. 2011.

[25] H. Huh, A. M. Tulino, and G. Caire, “Network MIMO with linear zero-forcing beamforming: large system analysis, impact of channel estimation and reduced-complexity scheduling,” *IEEE Trans. Inf. Theory*, vol. 58, no. 5, pp. 2911-2934, May 2012.

[26] R. Zakhour and S. V. Hanly, “Base station cooperation on the downlink: large system analysis,” *IEEE Trans. Inf. Theory*, vol. 58, no. 4, pp. 2079-2106, Apr. 2012.

[27] Y. Kim, J. Yang, and D. K. Kim, “A closed form approximation of the sum-rate upper bound of random beamforming,” *IEEE Commun. Lett.*, vol. 12, no. 5, pp. 365-367, May 2008.

[28] K.-H. Park, Y.-C. Ko, and M.-S. Alouini, “Accurate approximations and asymptotic results for the sum rate of random beamforming for multi-antenna Gaussian broadcast channels,” *in Proc. IEEE VTC 2009*, Apr. 2009.

[29] I. S. Gradshteyn and I. M. Ryzhik, *Table of Integrals, Series and Products*, 7th ed, A. Jeffrey and D. Zwillinger (Editors), Academic Press, 2007.

[30] J. L. Vicario, R. Bosisio, C. Anton-Haro, and U. Spagnolini, “Beam selection strategies for orthogonal random beamforming in sparse networks,” *IEEE Trans. Wireless Commun.*, vol. 7, no. 9, pp. 3385-3396, Sep. 2008.

[31] J. Wagner, Y. C. Liang, and R. Zhang, “On the balance of multiuser diversity and spatial multiplexing gain in random beamforming,” *IEEE Trans. Wireless Comm.*, vol. 7, no. 7, pp. 2512-2525, July 2008.

[32] M. Kountouris, D. Gesbert, and T. Salzer, “Enhanced multiuser random beamforming: dealing with the not-so-large number of users case,” *IEEE J. Sel. Area Commun.*, vol. 26, no. 8, pp. 1536 - 1545, Oct. 2008.

[33] J. W. Brown and R. V. Churchill, *Complex Variables and Applications*, 8th ed., Singapore: McGraw-Hill, 2009.

[34] H. David and H. Nagaraja, *Order Statistics*, 3rd ed., New York: Wiley, 2003.

[35] N. Jindal and A. Goldsmith, “Dirty-paper coding vs. TDMA for MIMO broadcast channels,” *IEEE Trans. Inf. Theory*, vol. 51, no. 5, pp. 1783-1794, May 2005.